Energy Engineering

Tech Science Press

DOI: 10.32604/ee.2024.055158

ARTICLE

Slag Characteristics of Biomass Pellet Fuels with Different Additives to Tobacco-Stalk for Tobacco Curing Heating

Jianan Wang[1,*], Yikuan Fan[2], Weidong Duan[3] and Zhaopeng Song[1]

[1]College of Tobacco Science, Henan Agricultural University, Zhengzhou, 450000, China

[2]China National Tobacco Corporation Henan Provincial Company, Zhengzhou, 450046, China

[3]Tobacco Production Department, China Tobacco Henan Industrial Co., Ltd., Zhengzhou, 450000, China

[*]Corresponding Author: Jianan Wang. Email: wangja@henau.edu.cn

Received: 19 June 2024 Accepted: 14 August 2024 Published: 21 October 2024

ABSTRACT

Since pure tobacco stalk (TS) biomass pellet fuels tend to slag, five anti-slagging agents were added to the crushed TS to obtain a pellet fuel that could be used in biomass burners to provide heat for tobacco curing. The obtained results revealed that the main component of TS pellet fuel was $K_2Si_2O_5$. During fuel combustion process, additives generated higher melting point silicate compounds by Al–K, Ca–K, and Ca–K elemental structures to replace single K elemental structure of TS, enhancing the anti-slagging efficiency of the pellet fuel from 21.63% to 78.29% and promoting the precipitation of K, Mg, and Na elements in the slag block. By investigating the anti-slagging mechanism pathways of the additives in TS biomass pellet fuels, altering of the structure of silicate ion group pathway was found to improve anti-slagging effects that met the requirements of production formula.

KEYWORDS

Pellet fuel; additives; flue-cured tobacco heating; potassium precipitation; silicate

Nomenclature

TS	Tobacco stalk
CMC	Carboxymethyl cellulose
KLN	Kaolin
DTE	Diatomaceous earth
CCO	Calcium carbonate
CHP	Calcium dihydrogen phosphate
XRD	X-ray diffraction
C_s	Slagging rate (%)
G_t	Total mass of the sampled furnace dust (kg)
G_1	Mass of slag with particle size >6 mm (kg)
η_e	Anti-slagging rate (%)
C_{TS}	Pure TS biomass pellet fuel slagging rate (%)
C_S	Slagging rates of different additive treatments (%)
η_K	Potassium fixation rate (%)
ω_1	Potassium contents in the slag after combustion pellet fuel (kg)

ω_2 Potassium contents in the original pellet fuel (kg)
η_o Oxygen enrichment rate (%)
ω_3 Oxygen contents in slag after combustion (kg)
ω_4 Oxygen contents in the original pellet fuel (kg)

1 Introduction

Flue-cured tobacco (*Nicotiana tabacum* L.) needs a great amount of energy for curing. In order to alleviate the environmental pollution due to traditional coal-fired heating, biomass pellet fuel has become popular for tobacco heating in recent years in China's tobacco growing regions [1]. To fully support sustainable development of energy-intensive agro-industry of tobacco flue-curing, over 4 million tons of biomass raw materials are employed annually to manufacture biomass pellet fuels [2]. Tobacco plants themselves can be developed as an energy crop for biofuels production [3]. Residual tobacco stalks from tobacco leaf harvests can be applied as a raw material for the production of biomass pellet fuel in tobacco plantations [4], which can potentially replace other biomass sources during heating process [5]. In this way, agricultural production of tobacco can be self-sustained [6], which is also the best approach to achieve green pathway obtaining of flue-cured tobacco [7].

Since TS have different structural composition from common agricultural crop straw [8], the pellet fuels made from this single-raw material is prone to furnace slagging when used in biomass burners for tobacco curing [9], which affects its combustion efficiency. To make it possible to use tobacco stalks (TS) pellet fuel in tobacco curing heating, Xiao et al. [10] tested flue-cured tobacco heating with biomass from TS samples from different locations, revealing the feasibility of using treated TS in traditional coal-fired furnaces. Due to the constraints of the production method at that time, pellet fuel with particle size φ 30–50 mm did not receive widespread promotion. With the development of modern science and technology, the burner used for tobacco has achieved automatic flame control and addition of pellet fuel with size φ 8–12 mm [11]. However, fuel combustion heating for tobacco leaf curing has its own rules based on changing dry-bulb temperature during curing process [12]. The slagging problem of single TS-based pellet fuels for flue-curing has not been perfectly resolved [13].

Today, crop straw, sawdust, or pulverized coal are commonly applied to alleviate furnace slagging problem [14]. However, differences in the regional distributions of these biomass raw materials increase fuel production cost [15], transportation energy consumption and equipment investment [16] due to long-distance transportation. At the same time, some researchers have performed in-depth analysis on the automation and intelligent control of biomass burners as well as pellet fuel particle size to address furnace slagging problem of TS fuels, though no significant results have been achieved [17].

Since additives have been successfully applied in mitigating slagging-related problems during solid fuel combustion [18] or in ash-forming species [19], Wang et al. [20] selected several anti-slagging agents and evaluated their application in tobacco curing heating process to potentially decrease the production cost of pellet fuel additives. However, limited research has been conducted on the composition and status of single TS-based pellet fuels for flue-curing. To decrease the slagging tendency of biomass pellet fuels of single TS, it is essential to identify the most suitable additives and develop anti-slagging mechanisms [21]. Based on previous research, this work aimed to quantitatively analyze the characteristics of the ash generated from TS-based pellet fuels by adding several common anti-slagging additives during tobacco curing heating process to provide a reference and further provide some directives for the screening process of TS-based pellet fuel additives.

2 Materials and Methods

2.1 Test Materials

The experiments were performed at Lushi Du-Guan Tobacco Planting Station in Henan Province from July to September in 2021–2022. With pure TS as control, carboxymethyl cellulose (CMC), calcium dihydrogen phosphate (CHP), calcium carbonate (CCO), diatomaceous earth (DTE), and kaolin (KLN) were selected as additives to be applied during tobacco curing process which were powder with 400 mesh, and came from Jintu Chemical Reagent Co., Ltd. (Zhengzhou, China). The addition proportions of these components are given in Table 1. TS samples were collected from Sheqi Yonghui Agricultural Cooperative and dried naturally. Then, they were crushed into particles less than 8 mm in length. Once the crushed TS material and different proportions of additives were evenly mixed, a pellet extruder (ZLG560, Jinan Xinyuanli Environmental Protection Equipment Co., Ltd., Jinan, China) was used to press them into a circular rod-shaped pellet fuel with a diameter of 8 mm, length of 2–3 times that of the diameter, particle density of 1200 kg/m^3, and bulk density of 650 kg/m^3. After the pressed pellet fuel was cooled down to room temperature, it was packed in waterproof sealed bags for experimental transportation and future application. The representative burner (SWZB223, Xuchuang Tongxing Modern Agricultural Technology Co., Ltd., Xuchang, China) [22] in China's tobacco planting regions applied for biomass pellet fuel was used to regularly feed the hopper with pellet fuel during the tobacco curing process. Then, the ash was cleaned and the obtained biomass pellet fuel was quantitatively detected and analyzed.

Table 1: Name and mixture ratio of anti-slagging additives

Treatment		Abbreviation	Ratio (wt%)
Name	Chemical structure		
Pure TS	Organic mixtures	TS	0%
Carboxymethyl cellulose	$[C_6H_7O_2(OH)_2OCH_2COONa]_n$	CMC	1%
Kaolin	$Al_2O_3{\cdot}2SiO_2{\cdot}2H_2O$	KLN	2%
Diatomaceous earth	$SiO_2{\cdot}nH_2O$	DTE	1%
Calcium carbonate	$CaCO_3$	CCO	2%
Calcium dihydrogen phosphate	$Ca(H)_2PO_4$	CHP	2%

2.2 Test Methods

2.2.1 Determination of Ash and Slag Compositions

To explore the slagging tendency of each treatment, the slagging rate of burner's ash was calculated by Eq. (1):

$$C_S = G_1/G_t \times 100\% \quad (1)$$

where C_S is slagging rate (%); G_t is total mass of the sampled furnace dust (kg); and G_1 is the mass of slag with particle size >6 mm (kg).

To compare anti-slagging degrees of different additives on pure TS, Eq. (2) was applied to calculate the efficiency of each treatment:

$$\eta_e = (C_{TS} - C_S) \ / \ C_{TS} \times 100\% \quad (2)$$

where η_e is anti-slagging rate (%); C_{TS} is pure TS biomass pellet fuel slagging rate (%); and C_S is the slagging rates of different additive treatments (%).

2.2.2 Determination of TS Slagging Temperature

To determine TS pellet fuel slagging temperature, a tubular combustion furnace (XD-1200NT; Zhengzhou Brothers Pit Furnace Co., Ltd., Zhengzhou, China) was applied for the simulation of biomass furnace combustion. In considering temperature range in biomass burner furnace during tobacco curing heating [23], temperature gradients were set as 900°C, 1000°C, 1100°C. The TS pellet particulate fuel was injected into the tubular combustion furnace to reach the specified temperature and keep it stable for 30 min. Once the temperature of the tubular combustion furnace was decreased to room temperature, the burnt products were collected for photographing and then, slagging conditions were observed. The combustion atmosphere of tubular combustion furnace was N_2 79 vol% + O_2 21 vol%, total flow was controlled at 2 L/min, and pressure was kept fixed at 0.1 MPa.

2.2.3 Scanning Electron Microscope-Energy-Dispersive Spectroscopy (SEM-EDS) and X-Ray Diffraction (XRD) Studies

A scanning electron microscope (SEM, Hitachi, S-4800, Tokyo, Japan) was applied to investigate the bonding mechanism and micro-morphology of crushed pellet fuels and slagging blocks by fracture surface analysis. In addition to SEM, an energy-dispersive spectroscope (EDS Hitachi, S-4800, Tokyo, Japan) was employed to investigate the representative areas scanned by an X-ray energy spectrometer to semi-quantitatively obtain detailed microchemistry information.

To reveal the influences of various treatments on the potassium content of pellet fuels during combustion, Eq. (3) was employed to calculate potassium fixation rate:

$$\eta_K = \omega_1 / \omega_2 \times 100\% \tag{3}$$

where η_K is potassium fixation rate (%) and ω_1 and ω_2 are potassium contents in the slag after combustion and in the original pellet fuel (kg), respectively.

To investigate the effect of oxygen content in particulate fuel during combustion, oxygen enrichment rate was calculated using Eq. (4) as:

$$\eta_o = (\omega_3 - \omega_4) / \omega_3 \times 100\% \tag{4}$$

where η_o is oxygen enrichment rate (%), and ω_3 and ω_4 are oxygen contents in slag after combustion and in the original pellet fuel (kg), respectively.

For the determination of the chemical composition of the slagging block after adding various additives, an X-ray diffraction (XRD) device (Fringe, LANScience, Shenzhen, China) was used for the identification of the main crystalline phases in slagging blocks after crushing. Then, the obtained data were analyzed with MDI Jade 6.5 software to qualitatively identify main crystalline phases [24].

2.3 Data Processing

GraphPad Prism software version 5.0 (GraphPad Software Company, San Diego, CA, USA) was applied for data analysis and automatic figure generation.

3 Results

3.1 Determination of TS Slagging Characteristics

Fig. 1 illustrates the combustion products of TS pellet fuel in the tubular combustion furnace. At 900°C and 1000°C, ash surface samples were soft and collapsed and pellet fuel did not form slag. At 1100°C, TS pellet fuel fiber structure was destroyed, rapidly shrinking with the burning of combustible components, and was agglomerated preventing dispersion. Hence, the products turned hard, forming black glass-like products attached to porcelain boat wall, which was difficult to take down, ultimately resulting in severe slagging. This revealed that the pellet fuel made from pure TS in the temperature range of 900°C–1100°C, it could not be used to supply the biomass burner system as temperature environment for tobacco curing is changing with the dry-bulb temperature of curing process.

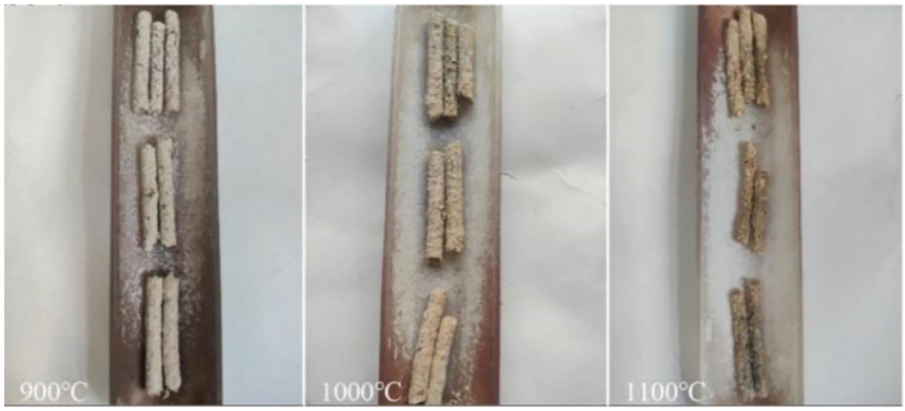

Figure 1: Morphology of combustion products of pure TS pellet fuel heated at different furnace temperatures

3.2 Characteristics of Ash and Slagging Blocks at Furnace Bottom during Tobacco Curing

In tobacco curing heating, TS slagging situation is more severe than other treatment methods (Fig. 2). This severe slagging could result in the accumulation of large blocks in pellet fuel burner furnace, thereby influencing normal pellet fuel feeding into the furnace, combustion air ventilation, and fuel combustion. According to the data presented in Fig. 1, the slagging statistics of various pellet fuels under various additive treatments during tobacco curing are illustrated in Figs. 3 and 4. Compared with only TS, addition of KLN and CHP additives to TS biomass pellet fuel was able to effectively control biomass pellet fuel slagging at 13.97% and 10.14%, respectively. As a whole, inorganic additives outperformed organic additives and increased anti-slagging rate by 21.63%–78.29% in varying degrees. Inorganic additive CHP presented good anti-slagging efficiency and could control slagging rate in furnace at 13.97%, reaching an anti-slagging rate of 78.29% and effectively alleviating TS-based pellet fuel slagging during tobacco curing process.

By investigating the elements present in various anti-slagging additives, the anti-slagging effects of alkali metals were ranked as CHP > KLN > CMC and for non-metallic element ions, the order was CHP > CCO > CMC, KLN > DTE, revealing that in anti-slagging additive selection for TS-based pellet fuels, the anti-slagging effects of additives containing high-molecular weight alkali metals and non-metallic elements (composed of oxidation ions) were better than those of additives containing low-molecular weight alkali metals and non-metallic elements (composed of oxidation ions).

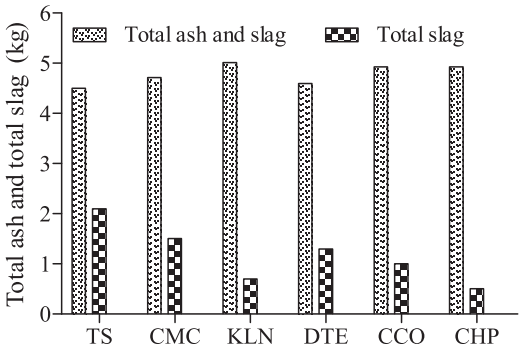

Figure 2: Comparison of ash and slagging of various additives during heating for tobacco curing

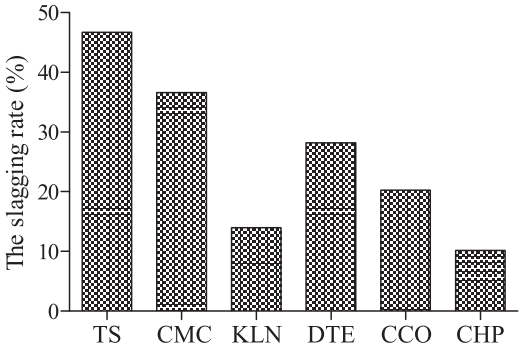

Figure 3: Comparison of slagging rates of various additives during heating for tobacco curing

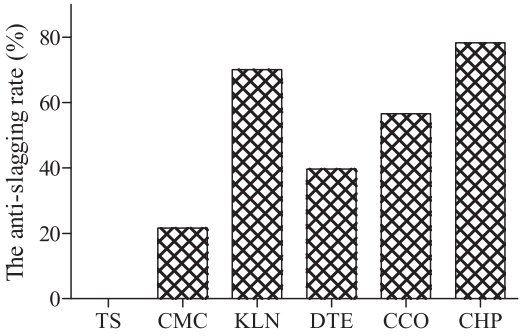

Figure 4: Comparison of anti-slagging rates of various additives during heating for tobacco curing

3.3 Analysis of Oxygen Enrichment and Potassium Fixation Rates in the Slagging Blocks of Different Additives

Fig. 5 comparatively analyzes the oxygen enrichment rates of various anti-slagging additives. Compared with raw materials, the oxygen content of slag exhibited more contrasting variations. KLN and CHP displayed positive values, while the other three showed negative values. Silicate is the general name for the compound formed by the combination of silicon, oxygen, and other chemical elements (such as Fe, Al, Mg, Ca, K, and Na) and its melting point is in the range of 1000°C–2000°C [25]. Based on the slagging situations of different fuels, as illustrated in Fig. 2, the addition of oxygen into the slag

promoted the combination of Si and O elements with $Si_xO_y^{z-}$ negative ion groups and formed silicate compounds with higher melting points with alkali metals, thus decreasing fuel slagging phenomenon during flue-cured tobacco heating process.

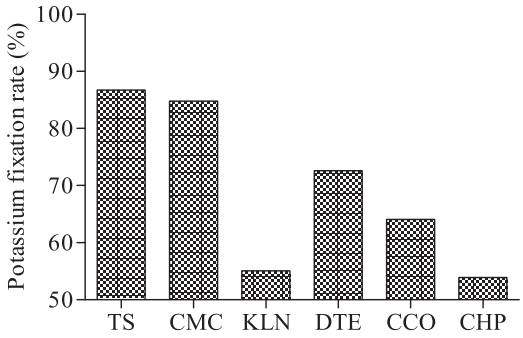

Figure 5: Comparison of potassium fixation rates of various anti-slagging additives

Fig. 6 compares the potassium fixation rates of various anti-slagging additives. The potassium fixation rates different additive treatments were decreased to varying degrees in the order of CMC > DTE > CCO > KLN > CHP. Compared with that of TS treatment, CMC treatment presented the highest potassium fixation rate of 84.78%, while addition of CHP and KLN significantly decreased fixation rate, reaching 53.89% and 55.07%, respectively.

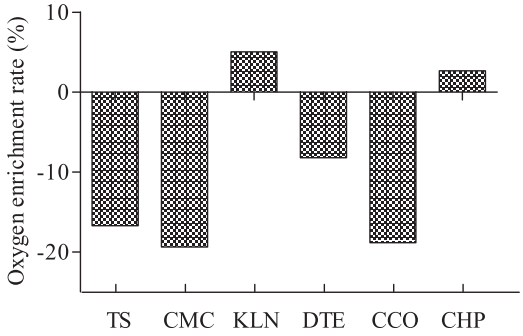

Figure 6: Comparison of oxygen enrichment rates of various anti-slagging additives

3.4 Analysis of Slagging XRD Spectra of Slagging Blocks with Different Additives

Fig. 7 illustrates the XRD patterns of the main residue crystals after particle combustion, which looked quite different from those of ordinary agricultural straws [24]. TS slag was primarily consisted of $K_2Si_2O_5$-based compounds with lower melting points. CMC slag was consisted of silicates such as Na_2SiO_3 and $Na_2O{\cdot}Al_2O_3{\cdot}6SiO_2$ and alkali metal oxides such as Na_2O, K_2O and $CaCO_3$. The main product of KLN slag was leucite ($KAlSi_2O_6$) mixed with Ca ($Al_2Si_3O_{10}$) and other high-melting point compounds. DTE slag was mainly consisted of $KAlSi_3O_8$- and $Mg_2Al_4Si_5O_{18}$-mixed structures and had high melting points. The main products of CCO slag were layered $K_2CaSi_4O_{10}$, $KAlSO_4$, and other medium-high melting point crystalline structures. CHP pellet fuel formed K–Al–Si compounds with high melting points, such as $KAlSi_3O_8$.

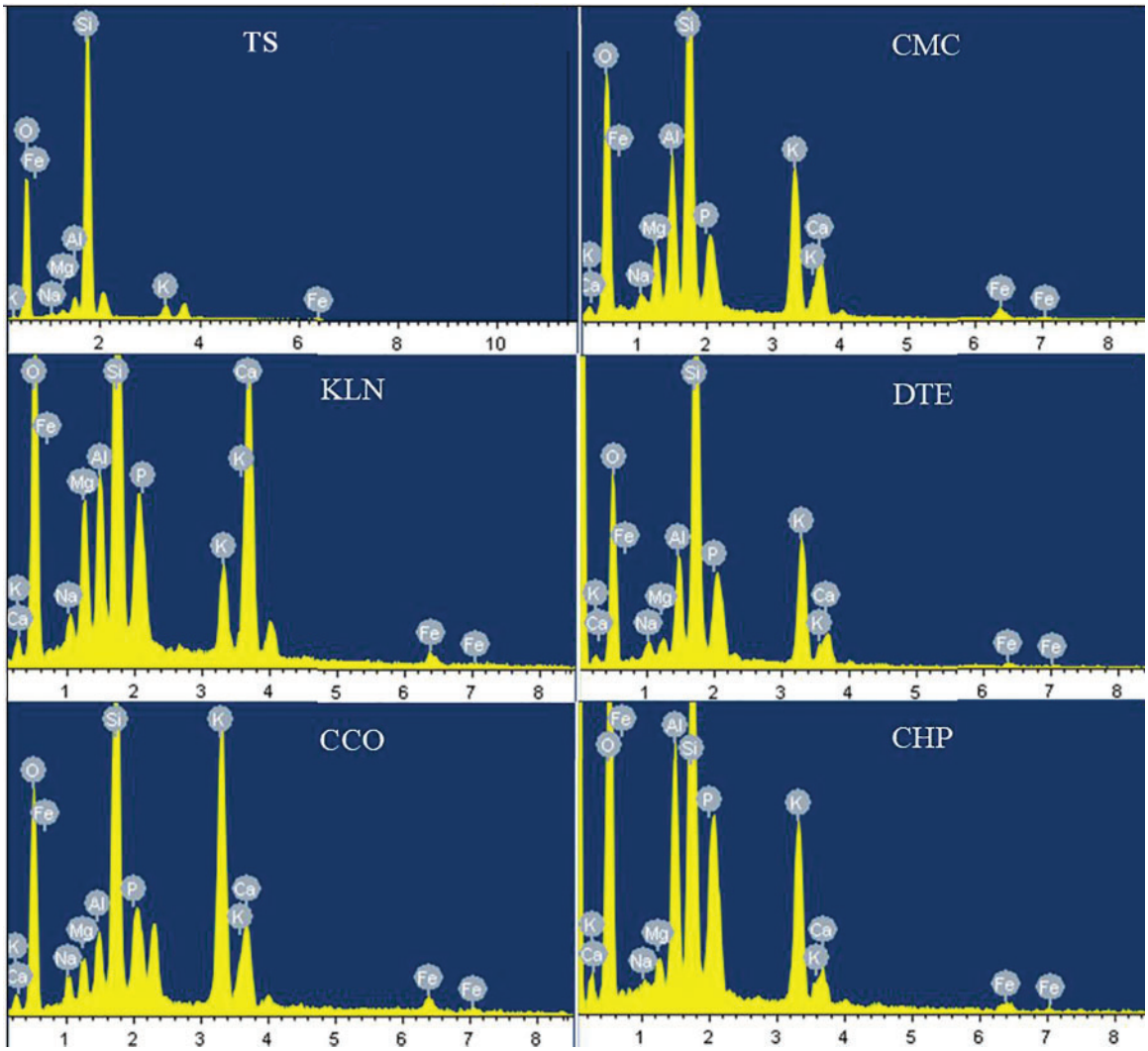

Figure 7: Slagging XRD patterns of various additives

3.5 SEM-EDS Analysis of Slagging Blocks

Fig. 8 shows the SEM images of the slagging blocks of various treatments with slagging particles having different appearances. TS slag lower surface was smooth and hard, possessing evident shrinkage pores due to sintering. The main elemental contents were O, Si, and K, with minor amounts of Mg, Al, and Fe. CMC slag blocks had block-like shapes, mainly represented by O, Si, K, Ca, Mg, and Na. KLN slag particles were cotton-like and their main representative elements were O, K, Si, Ca, and Al. DTE slagging particles presented irregular crystal structures, with the main representative elements being O, K, Si, Ca, and Mg. The ash particles of CCO were formed as agglomerated crystals and their main representative elements were O, Si, Ca, and K. The ash and slag particles of CHP combined together in irregular rod or block shapes. The main representative elements were Ca and P.

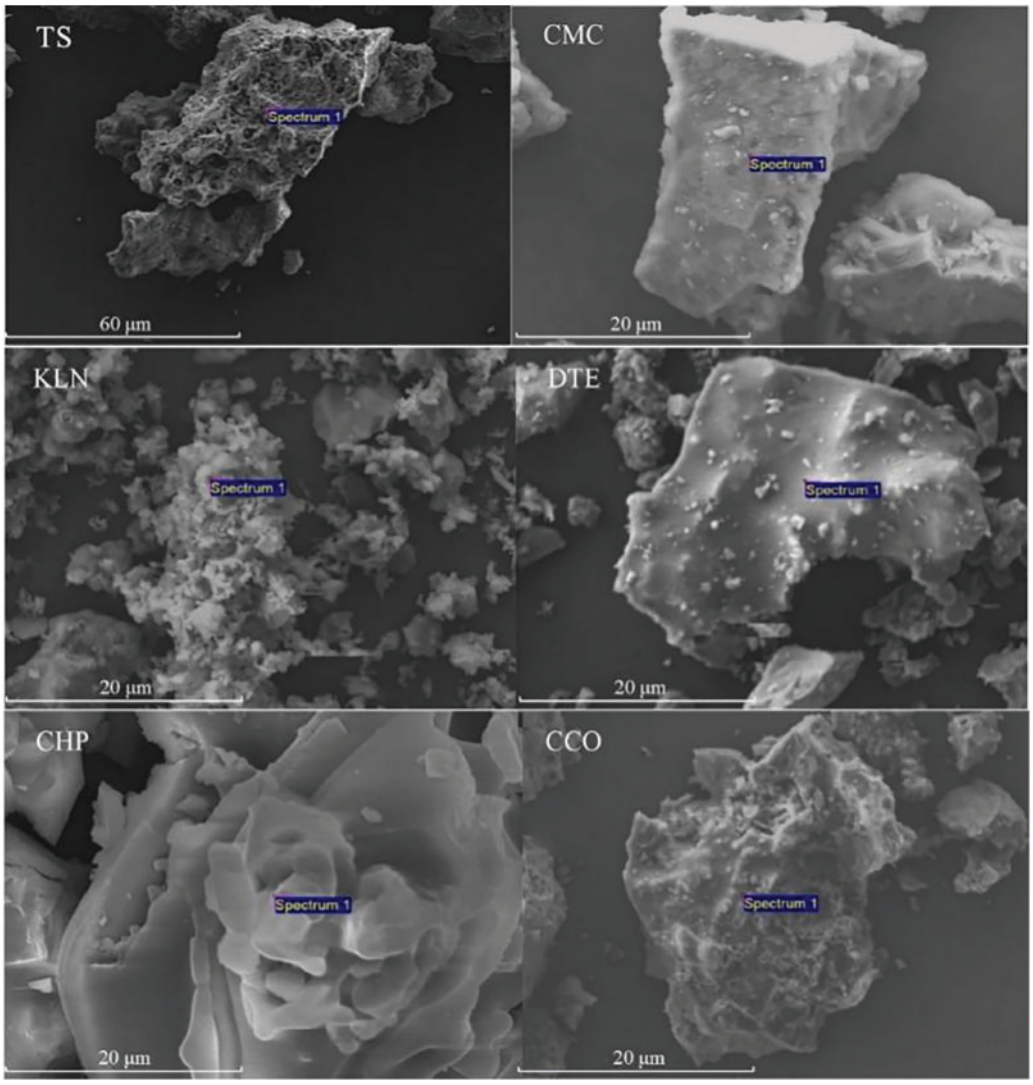

Figure 8: SEM images of the slagging contents of different additives

The EDS analyses of the slagging contents of various additives after complete TS pellet fuel combustion detected 23 elements (Table 2), with weight percentages ranging from 0.001% to 39.6%. Ca, O, K, and Si contents of the slags of various additive treatments accounted for more than 77.63% of their total content, with TS having the highest content of 82.68%. Comparison of the content changes of K, Mg, and Na elements in the slags of various additive treatments revealed that anti-slagging additives mainly decreased the contents of K, Mg, and Na in slags during combustion.

Table 2: EDS spot analysis results of SEM (wt%)

	TS	CMC	KLN	DTE	CCO	CHP
Ca	25.07	23.14	13.76	21.47	39.5	23.35
O	31.4	30.4	39.6	34.6	30.6	38.7
K	22.36	20.88	12.75	18.31	15.07	12.68
Si	3.85	3.37	12.53	7.632	2.51	2.9
Mg	4.01	3.91	2.29	3.94	3.2	2.97
Cl	3.87	5.8	2.31	3.26	2.43	1.69
P	2.92	2.73	1.8	2.94	1.99	13.14
S	2.641	2.523	1.66	2.44	1.76	2.12
Al	1.07	1.01	11.29	2.79	0.844	0.844
Na	1.19	4.86	0.645	1.07	0.935	0.704
Fe	1.17	1.04	0.74	1.08	0.853	0.648
Ti	0.12	0.114	0.397	0.18	0.08	0.075
Zn	0.0528	0.0476	0.0303	0.0466	0.04	0.0286
Sr	0.0901	0.0708	0.0622	0.0661	0.0685	0.0453
Ba	0.085	–	0.065	0.091	0.084	0.058
Mn	0.042	0.037	0.024	0.035	0.028	0.027
Cu	0.0352	0.028	0.0188	0.0262	0.021	0.0186
Rb	0.0164	0.0131	–	0.011	0.0119	–
Ce	0.051	–	–	–	–	–

Note: "–" Blank data.

3.6 Effects of Anti-Slagging Additives on the Transfer Pathways of Potassium and Silicon during Slagging

Based on the analyses presented in Figs. 1–8 and Table 2, the transfer paths of additives to slag silicon and potassium content of TS biomass pellet fuel were determined, as presented in Fig. 9. Slagging is reduced through three methods: (1) the pathway that facilitates the emission of potassium and chlorine (P–C–P pathway) by adding alkali metals and non-metallic negative ions to form low-melting point chloride, which are subsequently released out of furnace in the form of gas; (2) the pathway that decreases the potassium concentration of biomass pellet fuel (P–D pathway) by increasing other alkali metals (Fe, Na, and Mg) in granulation pellet fuel process, replacing single K element structure to generate silicate crystal structures with high melting points (Fe–K, Mg–K, and Na–K) by adding foreign substances to decrease S and K concentrations in the pellet fuel; and (3) the pathway that changes the structures of silicate ion groups (S–I–G pathway) by primarily changing the crystalline structures of silicic acid consisting of $Si_xO_y^{z-}$ negative ions in slagging materials. By increasing the y value or y to x ratio, high-melting point materials such as $Si_2O_6^{4-}$ and $Si_3O_8^{4-}$ form, improving anti-slagging efficiency. Furthermore, higher combination ability of phosphorus and potassium compared silicon [26] and high temperature stability of tar in $CaO–K_2O–P_2O_5$ ternary system [27] generate a mixture of K–Ca–P compounds, such as $K_2CaP_4O_{12}$, $K_2CaP_2O_7$, and $K_4Ca(PO_4)_2$ with high melting points, producing the other branch pathway caused by the phosphorus element of additives.

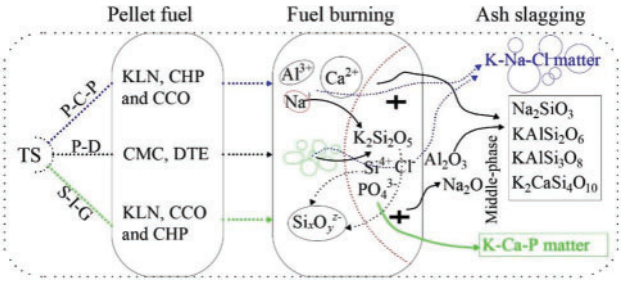

Figure 9: Effects of additives on the conversion paths of silicon and potassium during pellet fuel combustion

4 Discussion

The activity of alkali metals in TS pellet fuel combustion process directly affects the emission [28] and slagging of biomass combustion equipment [29]. In this research, the slagging rates of the burner's ash of various additive treatments were found to be proportional to their potassium fixation rates. As this is the pellet fuel combustion model for especial tobacco curing not to allow prediction of the temporal patterns of release of gas-phase potassium, it is not quite fit the traditional model for potassium release that is described by Mason et al. [30]. For example, low slagging rate of CHP corresponded to its low potassium fixation rate, while high slagging rate of TS corresponded to its high potassium fixation rate, indicating that anti-slagging additives applied to resist furnace slagging mainly decreased TS-based pellet fuel slagging rate by decreasing potassium fixation rate. The essential role of TS additives was possibly promoting the release of burning fuel in the form of gas from K, Mg, and Na elements during combustion, preventing the formation of low-melting point potassium silicates attached to burning pellet fuel and dust surface [31], and physically weakening further bonding and slagging of the contained substances. At fixed potassium content in TS-based pellet fuel during different test treatments, slagging blocks with low potassium fixation rates after combustion indicated that potassium was precipitated in the form of alkali metal gas or replaced with other alkali metals, which agreed with the findings of He et al. [22] using similar CHP TS additives.

Biomass burner furnace temperature in the heating chamber of flue-cured tobacco barn was 900°C–1100°C [25]. Chlorine species concentrations in flue gas and ash were clearly affected by combustion temperature [32]. Chlorine was released in the form of gas as HCl, NaCl, and KCl vapor at low temperatures [33] or during the case of low firepower [34]. At high temperatures, difference in emission profiles could be described in terms of K: (Si + Al) ratios, such that low (Si + Al) facilitated the release of KCl or KOH to gas phase [35]. In this research, chlorine element content variation patterns was closely related to slagging severity. It was found that three inorganic additives could decrease K: (Si + Al) ratios and were conducive to chlorine emission out of furnace.

Potassium content in tobacco straw was much higher than that in common crop straw and agricultural and forestry wastes [36]. In this research, TS pellet fuel slagging tendency was primarily caused by low-melting point silicates, mainly $K_2Si_2O_5$, condensed on ash surface. This was different from the furnace slagging of K_2CO_3 and K_2SO_4 generated from pure agricultural straw [37] and $CaCO_3$ produced after the combustion of sawdust, felling residue, and bark materials [38]. Hence, increasing potassium release in TS-based pellet fuel combustion process and reducing the production of low-melting point silicates should be the research directions for the selection of anti-slagging additives for TS, opposite to the improvement of potassium fixation rate in ash by crop straw additives [39]. The temperature and structure of furnace in biomass pellet fuel burners are key factors affecting biomass

particle slagging [40]. This research focused on heating environment in flue-cured tobacco curing. Further research is necessary on the slagging types of different anti-slagging TS-based pellet fuels in domestic or industrial boilers.

5 Conclusions

To determine flue-curing TS slagging conditions and the properties of its residues, five anti-slagging additives with different proportions were added to TS to create biomass pellet fuel. A representative biomass burner to cure tobacco with heat was applied for flue-curing and a certain amount of slagging residue was analyzed. The obtained results revealed that TS pellet fuel residue was mainly consisted of low-melting point $K_2Si_2O_5$.

In summary, the anti-slagging mechanism proposed in this research using various additives showed that: 1) Increase of potassium precipitation promoted the release of K, Mg, and Na in pellet fuel during combustion. Lower potassium fixation rates of different slag treatments resulted in more obvious anti-slagging effects. 2) Alkali metals in the additives replaced silicates with K structures in TS pellet fuels to generate silicates with high melting points of Al–K, Ca–K, Fe–K, Mg–K, and Na–Na structures. 3) The structure of silicate functional groups from simple $Si_2O_5^{2-}$ was reconstructed into complex $Si_xO_y^{z-}$ with high melting point.

Acknowledgement: This study was funded by Henan China Tobacco Industry Co., Ltd. and Henan Provincial Tobacco Company.

Funding Statement: This study was funded by Henan China Tobacco Industry Co., Ltd. (Grant No. 2022410000340099) and Henan Provincial Tobacco Company (Grant No. 2018410000270097).

Author Contributions: Study conception and design: Jianan Wang and Zhaopeng Song; data collection: Yikuan Fan; analysis and interpretation of results: Jianan Wang and Weidong Duan; draft manuscript preparation: Jianan Wang. All authors reviewed the results and approved the final version of the manuscript.

Availability of Data and Materials: This statement should make clear how readers can access the data used in the study and explain why any unavailable data cannot be released. The data that support the findings of this study are available from *China National Tobacco Corporation* but restrictions apply to the availability of these data, which were used under license for the current study, and so are not publicly available. Data are however available from the authors upon reasonable request and with permission of *China National Tobacco Corporation*.

Ethics Approval: This study did not involve human or animal subjects.

Conflicts of Interest: The authors declare that they have no conflicts of interest to report regarding the present study.

References

[1] X. Qin, S. Y. Yao, Z. F. Wang, X. M. Tang, W. Yao and C. G. Fu, "Effect of low temperature and low HUMIDITY curing technique based on biomass fuel on the quality of Yuyan 87 tobacco," (in Chinese), *Crop Res.*, vol. 36, no. 6, pp. 546–550, Dec. 2022. doi: 10.16848/j.cnki.issn.1001-5280.2022.06.09.

[2] J. A. Wang, Q. Zhang, Y. W. Wei and G. H. Yang, "Integrated furnace for combustion/gasification of biomass fuel for tobacco curing," *Waste Biomass Valor.*, vol. 10, no. 7, pp. 2037–2044, Jul. 2019. doi: 10.1007/s12649-018-0205-1.

[3] F. G. Barla and S. Kumar, "Tobacco biomass as a source of advanced biofuels," *Biofuels*, vol. 10, no. 3, pp. 335–346, Jul. 2019. doi: 10.1080/17597269.2016.1242684.

[4] P. D. de Souza, T. L. Badin, D. L. Pasa, M. C. Ximendes and J. A. de Farias, "Analysis of energy sufficiency in a family farming production chain," *Rev. Arvore*, vol. 47, no. 10, Oct. 2023. doi: 10.1590/1806-908820230000014.

[5] B. Palupi, B. A. Fachri, I. Rahmawati, M. F. Rizkiana and H. W. Amini, "Pretreatment of tobacco stems as bioethanol raw material: The effect of temperature and time using chemical method," *AIP Conf. Proc.*, vol. 2278, 2020, Art. no. 020023. doi: 10.1063/5.0014558.

[6] T. B. Ren *et al.*, "Application of biomass moulding fuel to automatic flue-cured tobacco furnaces efficiency and cost-effectiveness," *Therm. Sci.*, vol. 23, no. 5, pp. 2667–2675, Oct. 2019. doi: 10.2298/TSCI181202156R.

[7] M. Bortolini, M. Gamberi, C. Mora and A. Regattieri, "Greening the tobacco flue-curing process using biomass energy: A feasibility study for the flue-cured Virginia type in Italy," *Int. J. Green Energy*, vol. 16, no. 14, pp. 1220–1229, Sep. 2019. doi: 10.1080/15435075.2019.1671397.

[8] J. H. Pan, M. Y. Wang, X. Z. Shi, J. Z. Yang, X. Q. Xie and Y. T. Tian, "Nitrification egulation by a new organic compost in ultisols of a flue-cured tobacco plantation," *Commun. Soil Sci. Plant Anal.*, vol. 54, no. 21, pp. 3006–3018, Nov. 2023. doi: 10.1080/00103624.2023.2253844.

[9] S. Mukhopadhyay, R. E. Masto, P. Sarkar and S. Bari, "Biochar washing to improve the fuel quality of agro-industrial waste biomass," *J. Energy Inst.*, vol. 102, no. 3, pp. 60–69, Mar. 2022. doi: 10.1016/j.joei.2022.02.011.

[10] X. D. Xiao, C. M. Li, P. Ya, J. He, Y. S. He and X. T. Bi, "Industrial experiments of biomass briquettes as fuels for bulk curing barns," *Int. J. Green Energy*, vol. 12, no. 11, pp. 1061–1065, Jul. 2015. doi: 10.1080/15435075.2014.891119.

[11] J. A.Wang, Y. K. Fan, Z. B. Zhao, J. J. Liu, C. P. Song and F. J. Wei, "Performance of biomass fuel pellets of different sizes in combustion heating for tobacco flue-curing," *J. Environ. Prot. Ecol.*, vol. 23, no. 3, pp. 1031–1038, Jun. 2022.

[12] J. X. Jia, M. J. Zhang, J. C. Zhao, J. A. Wang, F. He and L. F. Wang, "The effects of increasing the dry-bulb temperature during the stem-drying stage on the quality of upper leaves of flue-cured tobacco," *Process*, vol. 11, no. 3, pp. 1–11, Mar. 2023. doi: 10.3390/pr11030726.

[13] Z. D. Qiu, Y. C. Lian, Y. Lu, X. Wang, M. G. Lin and Q. T. Lin, "Application of tobacco stem and sawdust formulated biomass fuel in tobacco curing," *J. Fujian Agric. For. Univ. (Nat. Sci. Ed.)*, vol. 50, no. 1, pp. 10–15, Jan. 2021. doi: 10.13323/j.cnki.j.fafu(nat.sci.).2021.01.002.

[14] M. Liang *et al.*, "Physical and combustion properties of binder-assisted hydrochar pellets from hydrothermal carbonization of tobacco stem," *Waste Biomass Valor.*, vol. 11, no. 11, pp. 6369–6382, Nov. 2020. doi: 10.1007/s12649-019-00848-x.

[15] K. Y. Tippayawong, N. Chaidi, T. Ngamlertsappakit and N. Tippayawong, "Demand and cost analysis of agricultural residues utilized as biorenewable fuels for power generation," *Energy Rep.*, vol. 6, no. 9, pp. 1298–1302, Jan. 2020. doi: 10.1016/j.egyr.2020.11.040.

[16] W. R. Cervi *et al.*, "Mapping the environmental and techno-economic potential of biojet fuel production from biomass residues in Brazil," *Biofuels Bioprod. Bioref.-Biofpr*, vol. 15, no. 1, pp. 282–304, Jan. 2021. doi: 10.1002/bbb.2161.

[17] Z. P. Song, F. J. Wei, X. F. Su, Y. J. Wang, Y. K. Fan and J. A. Wang, "Application of automatic control furnace for combustion of biomass briquette fuel for tobacco curing," *Thermal Sci.*, vol. 25, no. 4, pp. 2425–2435, Aug. 2021. doi: 10.2298/TSCI191115148S.

[18] H. Ghazidin, S. Suyatno, A. Prismantoko and F. Karuana, "Impact of additives in mitigating ash-related problems during co-combustion of solid recovered fuel and high-sulfur coal," *Energy*, vol. 292, Sep. 2024, Art. no. 130510. doi: 10.1016/j.energy.2024.130510.

[19] J. L. Míguez, J. Porteiro and F. Behrendt, "Review of the use of additives to mitigate operational problems associated with the combustion of biomass with high content in ash-forming species," *Renew. Sustain. Energy Rev.*, vol. 141, no. 2, pp. 4941–4946, Feb. 2021. doi: 10.1016/j.rser.2020.110502.

[20] L. Wang, Y. K. Fan, F. He, B. Q. Niu, F. J. Wei and H. B. Zhao, "Screening and testing of anti-slagging agents for tobacco-stalk-based biomass pellet fuel for tobacco curing," *Processes*, vol. 10, no. 9, pp. 1690–1701, Sep. 2022. doi: 10.3390/pr10091690.

[21] P. Bareschino, E. Marrasso and C. Roselli, "Tobacco stalks as a sustainable energy source in civil sector: Assessment of techno-economic and environmental potential," *Renew. Energy*, vol. 175, no. 9, pp. 373–390, Sep. 2021. doi: 10.1016/j.rser.2020.110502.

[22] F. He, F. J. Wei, C. J. Ma, H. B. Zhao, Y. K. Fan and L. F. Wang, "Performance of an intelligent biomass fuel burner as an alternative to coal-fired heating for tobacco curing," *Pol. J. Environ. Stud.*, vol. 30, no. 1, pp. 134–140, Feb. 2021. doi: 10.15244/pjoes/122164.

[23] J. A. Wang, Y. K. Fan, T. Q. Zhang, F. J. Wei, H. B. Zhao and L. He, "Design and test of biomass furnace in intensive baking room," *Acta Tabacaria Sin.*, vol. 27, no. 4, pp. 36–44, Jul. 2021. doi: 10.16472/j.chinatobacco.2021.027.

[24] Q. Wang, K. H. Han, J. M. Wang, J. Gao and C. M. Lu, "Influence of phosphorous based additives on ash melting characteristics during combustion of biomass briquette fuel," *Renew. Energy*, vol. 113, no. 12, pp. 428–437, Dec. 2017. doi: 10.1016/j.renene.2017.06.018.

[25] L. Wang, M. Becidan and Φ. Skreiberg, "Sintering behavior of agricultural residues ashes and effects of additives," *Energy Fuels*, vol. 26, no. 9, pp. 5917–5929, Sep. 2012. doi: 10.1021/ef3004366.

[26] F. H. Li, B. Yu, W. Zhao, W. J.Wang, M. L. Xu and H. L. Fan, "Investigation on formation mechanisms of ash and deposit from cotton stalk vibrating grate boiler combustion based on their characteristics," *Fuel*, vol. 232, no. 5, May 2022, Art. no. 124446. doi: 10.1016/j.fuel.2022.124446.

[27] P. Billen, J. Van Caneghem and C. Vandecasteele, "Predicting melt formation and agglomeration in fluidized bed combustors by equilibrium calculations," *Waste Biomass Valor.*, vol. 5, no. 5, pp. 879–892, Oct. 2014. doi: 10.1007/s12649-013-9285-0.

[28] A. V. Kovekhova, O. D. Arefieva, N. A. Didenko and L. A. Zemnukhova, "Composition of inorganic components in Helianthus tuberosus stems," *Izvestiâ vuzov. Prikladnaâ himiâ i biotehnologiâ*, vol. 11, no. 2, pp. 299–309, Jul. 2021. doi: 10.21285/2227-2925-2021-11-2-299-309.

[29] Y. P. Zhang, B. S. Jin and R. P. Liu, "Factors affeceting alkali release and transformation during corncob combustion," *ACTA Energiae Solaris Sin.*, vol. 30, no. 2, pp. 129–133, Feb. 2009.

[30] P. E. Mason, J. M. Jones and L. I. Darvell, "Gas phase potassium release from a single particle of biomass during high temperature combustion," *Proc. Combustion Inst.*, vol. 36, no. 2, pp. 2207–2215, Jan. 2017. doi: 10.1016/j.proci.2016.06.020.

[31] Q. Wang, K. H. Han, P. F. Wang, S. J. Li and M. Zhang, "Influence of additive on ash and combustion characteristics during biomass combustion under O_2/CO_2 atmosphere," *Energy*, vol. 195, no. 5, pp. 4941–4946, May 2020. doi: 10.1016/j.energy.2020.116987.

[32] L. C. R. Sá, L. M. E. F. Loureiro and L. J. R. Nunes, "Torrefaction as a pretreatment technology for chlorine elimination from biomass: A case study using *Eucalyptus globulus* labill," *Resources*, vol. 9, no. 5, May 2020. doi: 10.3390/resources9050054.

[33] H. Kaufmann and T. Nussbaumer, "Formation and behaviour of chlorine compounds during biomass combustion," *Gefahrstoffe Reinhaltung Der Luft*, vol. 59, no. 7–8, pp. 267–272, Jul.–Aug. 1999.

[34] J. Wojciech and K. Monika, "Examination of inorganic gaseous species and condensed phases during coconut husk combustion based on thermodynamic equilibrium predictions," *Renew. Energy*, vol. 167, no. 6, pp. 497–507, Jan. 2021. doi: 10.1016/j.renene.2020.11.105.

[35] D. S. Clery, P. E. Mason and C. M. Rayner, "The effects of an additive on the release of potassium in biomass combustion," *Fuel*, vol. 214, no. 2, pp. 647–655, Feb. 2018. doi: 10.1016/j.fuel.2017.11.040.

[36] H. X. Zhang, F. Y. Wu, Y. L. Chen, Z. X. He, Q. L. Zhu and Y. L. Mao, "Effects of tobacco stem-derived biochar on different forms of soil potassium and photosynthetic characteristics of tobacco," (in Chinese), *J. Fujian Agric. For. Univ. (Nat. Sci. Ed.)*, vol. 51, no. 4, pp. 468–477, Jul. 2022. doi: 10.13323/j.cnki.j.fafu(nat.sci.).2022.04.004.

[37] Q. Wang, K. H. Han and P. F. Wang, "Influence of phosphorus-based additives on potassium transformation during pyrolysis and ash characteristics of biochar briquettes," *Bioenergy Res.*, vol. 13, no. 3, pp. 907–917, Sep. 2020. doi: 10.1007/s12155-020-10118-7.

[38] M. Öhman, C. Bomana, H. Hedman, A. Nordin and D. Boström, "Slagging tendencies of wood pellet ash during combustion in residential pellet burners," *Biomass Bioenergy*, vol. 27, no. 6, pp. 585–596, Jan. 2004. doi: 10.1016/j.biombioe.2003.08.016.

[39] Q. Wang, K. H. Han, J. H. Qi, J. G. Zhang, H. P. Li and C. M. Lu, "Investigation of potassium transformation characteristics and the influence of additives during biochar briquette combustion," *Fuel*, vol. 222, no. 6, pp. 407–415, Jun. 2018. doi: 10.1016/j.fuel.2018.02.156.

[40] S. J. Xiong, J. Burvall, H. Örberg, G. Kalen, M. Thyrel and M. Öhman, "Slagging characteristics during combustion of corn stovers with and without kaolin and calcite," *Energy Fuels*, vol. 22, pp. 2465–2470, Sep.–Oct. 2008. doi: 10.1021/ef700718j.